Synchronization in Small-World Systems

Mauricio Barahona[1,2] and Louis M. Pecora[3]
[1]Control and Dynamical Systems, California Institute of Technology, Pasadena, California 91125
[2]Department of Bioengineering, Imperial College, London SW7 2BX, United Kingdom
[3]Naval Research Laboratory, Code 6340, Washington, D.C. 20375
(Received 17 December 2001; published 16 July 2002)

We quantify the dynamical implications of the small-world phenomenon by considering the generic synchronization of oscillator networks of arbitrary topology. The linear stability of the synchronous state is linked to an algebraic condition of the Laplacian matrix of the network. Through numerics and analysis, we show how the addition of random shortcuts translates into improved network synchronizability. Applied to networks of low redundancy, the small-world route produces synchronizability more efficiently than standard deterministic graphs, purely random graphs, and ideal constructive schemes. However, the small-world property does not guarantee synchronizability: the synchronization threshold lies within the boundaries, but linked to the end of the small-world region.

DOI: 10.1103/PhysRevLett.89.054101 PACS numbers: 05.45.–a, 89.75.–k

Recently, Watts and Strogatz [1] showed that the addition of a few long-range shortcuts to an otherwise locally connected lattice sharply reduces the average distance between nodes while the system is still relatively localized. The ensuing semirandom lattice was denoted a small world (SW). This concept had immediate resonance in a variety of disciplines dealing with the analysis and design of complex networks. Even more so because the SW property seems to be a quantifiable (and intuitive) characteristic of many real-world structures [1–4], both human-generated (social networks, WWW, power grid), or of biological origin (neural and biochemical networks). Ongoing research has focused on static and combinatoric properties [2,5–10] of a tractable SW model [1,11]. Closer to our work, Monasson [11] considered the SW effect on spectra of connectivity matrices relevant in condensed matter and polymer physics [12].

Underlying this research is the implication that the structural properties of a network must have some bearing on the dynamics taking place on it [2]. However, despite their widespread importance, there has been little (mostly numerical) work dealing explicitly with dynamical processes on small worlds. Among those, simulations of automata epidemics [13] and Web browsing [14], and numerical studies of synchronization in continuous and discrete systems [3,15–17]. These few examples indicate improved SW synchronization or coherence for these specific models, but provide neither a generic picture nor systematic insight into how the SW property influences the prevalent phenomenon of network synchronization. Moreover, some of the conclusions drawn from the numerics are partial and based on entrenched misconceptions. In particular, the statement that synchronization is made possible by *any* amount of added random shortcuts [16,17], is nongeneric as it ignores the nonintuitive, yet common, situation in which synchronicity may be lost by increasing the coupling between oscillators [18–20].

Our aim is to link explicitly the SW addition of random shortcuts to the synchronization of networks of coupled dynamical systems. This is an example of dynamics *on* networks—leaving aside the distinct problem of evolution *of* networks here. We rely on a generic formulation [18–21] which allows us to factor out the connectivity content, and thus identify the synchronization threshold (a dynamic attribute) with an algebraic property of the Laplacian matrix of the graph. We then quantify both numerically and analytically how the SW scheme improves the synchronizability of the network. In the context of network design, the semirandom SW strategy is shown to be an efficient way of producing synchronizable networks when compared to standard deterministic graphs and even to fully random or ideal constructive schemes. We also find that the synchronization threshold lies in the SW region [3,13], but does not coincide with its onset—in fact, it is linked to the effective randomization that ends SW. In other words, the small-world property does not guarantee in general that a network will be synchronizable.

We keep the formalism to a minimum. Consider n identical dynamical systems $\{\mathbf{x}^i, i = 1, \ldots, n\}$ (placed at the nodes of a graph) that are linearly and symmetrically coupled with global coupling σ, as represented by the edges of the undirected graph. The graph topology is encoded in the Laplacian G, a symmetric matrix with zero row-sum and real spectrum [22]. The equations of motion are the following: $\dot{\mathbf{x}}^i = \mathbf{F}(\mathbf{x}^i) + \sigma \sum_{j=1}^{n} G_{ij}\mathbf{H}(\mathbf{x}^j)$, with $\mathbf{H}$ an output function—the same at each node. To assess the linear stability of the synchronous state $\{\mathbf{x}^i = \mathbf{s}, \forall i\}$, we need to diagonalize the variational equations $\dot{\xi}^i = \sum_j [\delta_{ij} D\mathbf{F}(\mathbf{s}) + \sigma G_{ij} D\mathbf{H}(\mathbf{s})]\xi^j$, and check that the perturbations transverse to the synchronization manifold are damped. The importance of the network topology comes now to fore. The diagonalization of G transforms the variational equations into n blocks of the form: $\dot{\zeta}^l = [D\mathbf{F}(\mathbf{s}) + \sigma\theta_l D\mathbf{H}(\mathbf{s})]\zeta^l$, which only differ in

 0031-9007/02/89(5)/054101(4)$20.00

$\{\theta_l, l = 0, \ldots, n-1\}$, the eigenvalues of the topology matrix G. The synchronous state, linked to $\theta_0 = 0$, is stable if the remaining $(n-1)$ blocks, associated with graph eigenmodes transverse to the synchronization manifold, have negative Lyapunov exponents.

The last piece in the analysis is the stability plot of the maximum Lyapunov exponent $\lambda_{\max}$ vs generic coupling α for the particular functions **F** and **H** at the nodes. Several cases of $\lambda_{\max}$, called the *master stability function* [18–21], are shown in Fig. 1. Crucially, a large class of oscillatory systems (periodic, quasiperiodic, and even chaotic dominated by a few unstable periodic orbits) have master stability functions with the generic characteristics depicted in Fig. 1. Noting that the variational blocks ζ are just scaled by the graph eigenvalues θ_l, we obtain the generic requirement for the synchronous state to be linearly stable: $\sigma\theta_l \in (\alpha_1, \alpha_2)$, i.e., *all* the eigencouplings $\sigma\theta_l$ must be located in the negative region of the master stability function. Figure 1 illustrates the intricacies of this criterion. Increasing the coupling α from zero produces a decrease of $\lambda_{\max}$, which tends to induce stability ($\lambda_{\max} < 0$) . However, further increases in coupling may cause destabilization of the synchronous state ($\lambda_{\max} > 0$). Hence, contrary to claims in [16,17], increasing the global coupling σ until $\sigma\theta_l \geq \alpha_1$ is not sufficient to guarantee synchronicity, since it may not be possible to fit all the eigencouplings in the deep, stable region of $\lambda_{\max}$. This can be expressed as an algebraic condition for the existence of a linearly stable synchronous state: a network is synchronizable if

$$\theta_{\max}/\theta_1 < \alpha_2/\alpha_1 \equiv \beta, \tag{1}$$

where θ_1 is the first nonzero eigenvalue (FNZE) and $\theta_{\max}$ is the maximum eigenvalue of the Laplacian G. The figure of merit β, which encapsulates the properties of the node

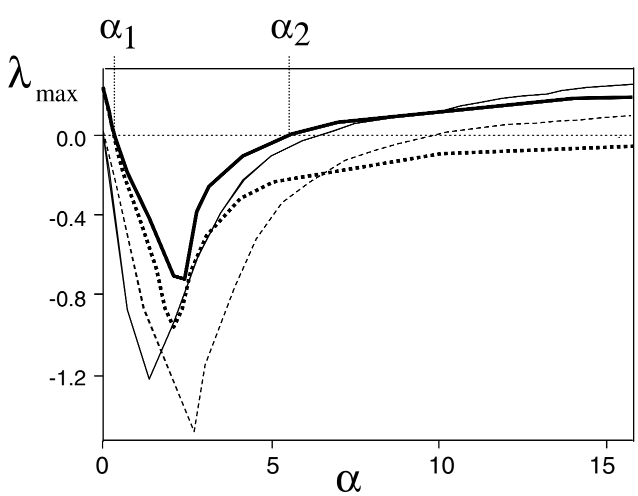

FIG. 1. Four typical master stability functions for coupled Rössler oscillators: chaotic (bold) and periodic (regular lines); with y coupling (dashed) and x coupling (solid lines). (All scaled for clearer visualization.) We concentrate on the x-coupled chaotic case with a negative region (α_1, α_2).

dynamics, ranges from 5 to 100 for a variety of chaotic oscillators (e.g., Lorenz, Rössler, double-scroll). The eigenratio condition (1) has an important implication: some networks are just not synchronizable no matter how the global coupling σ is tuned [23].

In this light, we explore the impact of the SW property on synchronizability. For concreteness, consider in what follows a network of x-coupled standard Rössler chaotic oscillators [18,20], with $\beta \simeq 37.85$. Small worlds are generated by adding random connections to a "pristine world," a cycle of n nodes each coupled to its $2k$ nearest neighbors for a total of nk edges [11]. Like other local lattices, pristine worlds are difficult to synchronize because their eigenratio increases rapidly with n. This can be seen by Fourier-diagonalizing the Laplacian G^0 of a pristine world, a banded circulant matrix with $(2k)$ on the main diagonal and (-1) on the $2k$ (circulantly) adjacent diagonals, to obtain its spectrum [11,24]:

$$\theta_1^0 \simeq 2\pi^2 k(k+1)(2k+1)/3n^2, \qquad k \ll n, \tag{2}$$

$$\theta_{\max}^0 \simeq K + \csc(3\pi/2K) \simeq K(1 + 2/3\pi), \quad k \gg 1, \tag{3}$$

$$\theta_{\max}^0/\theta_1^0 \simeq (3\pi+2)n^2/[2\pi^3 k(k+1)]. \tag{4}$$

where $K = 2k+1$. The large eigenratio (4) leads to poor synchronizability. From (1), the maximum number of x-coupled Rössler oscillators that can be synchronized in a simple cycle configuration (a pristine world of $k = 1$) is only 19. This number increases to 34 if we add connections to the second nearest neighbors ($k = 2$). Synchronizability can be steadily improved through the addition of edges in such a deterministic scheme until we reach the totally connected graph ($k = \lceil n/2 \rceil$), which is synchronizable for all n. In general, n nodes can be synchronized in a pristine world arrangement if $k > k_{\min}^0 \simeq n\sqrt{(3\pi+2)/(2\pi^3\beta)} \simeq 0.429\beta^{-1/2}n$.

Clearly, this is not an efficient route to synchronizability if connections are counted as a cost. Purely random graphs $\mathcal{G}_{n,f}$, in which a fraction f of the $n(n-1)/2$ possible edges is picked at random, drop below the synchronization threshold with fewer connections (on average). With eigenratio [22]

$$\frac{\theta_{\max}^{RG}}{\theta_1^{RG}} \simeq \frac{nf + \sqrt{2f(1-f)n\ln n}}{nf - \sqrt{2f(1-f)n\ln n}}, \tag{5}$$

they reach synchronizability just after they become "almost surely" connected at $f \simeq 2\ln n/(n + 2\ln n)$. However, disconnectedness means unsynchronizability ($\theta_1^{RG} = 0$) when the number of edges is below $\sim n\ln n$. In addition to this limitation, random graphs are costly to store in the sense of algorithmic incompressibility.

Figure 2 illustrates the advantages of the semirandom SW as compared to the deterministic and purely random schemes [25]. Small worlds are obtained by doping a pristine world (with nk edges) through the addition of ns edges picked at random from the $n(n-2k-1)/2$ remaining pairs. The average number of shortcuts per node (s) is

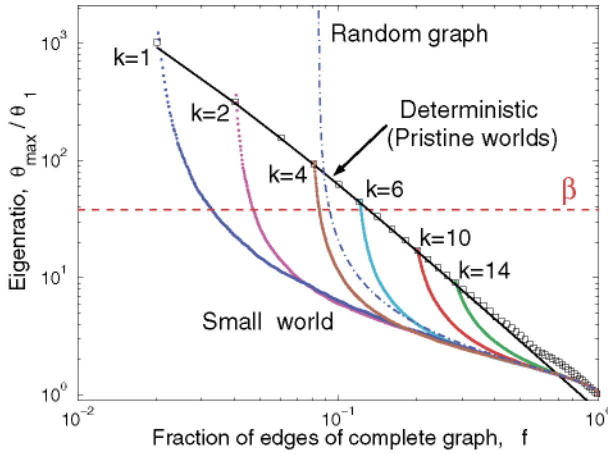

FIG. 2 (color online). Decay of the eigenratio in a $n = 100$ lattice as $f\binom{n}{2}$ edges are added following purely deterministic, semirandom (SW), and purely random schemes. Networks become synchronizable below the dashed line (β). The squares (numerical) and the solid line [analytic Eq. (4)] show the eigenratio decay of pristine worlds through the deterministic addition of short-range connections. The dot-dashed line corresponds to purely random graphs [Eq. (5)], which become *almost surely* disconnected and unsynchronizable at $f \simeq 0.0843$. The semirandom SW approach (dots, shown for ranges $k = 1, 2, 4, 6, 10, 14$) is more efficient in producing synchronization when $k < \ln n$.

related to previous measures [1,11] of randomness (p and q): $s \equiv kp \equiv q(n - 2k - 1)/(2n)$. As shortcuts are added, the eigenratio drops sharply until the network becomes synchronizable above a threshold s_{sync} where (1) is fulfilled. Note that the SW approach is more efficient than deterministically adding short-range layers, and it also ensures synchronizability when random graphs are below their percolating transition. Interestingly, adding many shortcuts beyond the initial drop brings in little extra stability, but it buys robustness. As the number of added shortcuts grows, the synchronization behaviors of SW and random graphs converge. This is, in dynamical terms, the effective randomization of the network through SW addition. This randomized region is *robust* to edge deletion: not until over 90% are cut (for k small) does the eigenratio change drastically. All of this suggests that a SW scheme applied to pristine worlds of low redundancy ($k < \ln n$) is a plausible strategy to generate synchronizable networks.

To make these ideas more precise, we show in Fig. 3 the minimum number of edges needed for synchronizability in different configurations. As stated above, pristine worlds need $f^0_{\mathrm{min}} \to 0.858/\sqrt{\beta} \simeq 0.140$, a constant fraction of the edges of the complete graph. This scales like $\sim n^2$ and, in this sense, the cost of synchronization is high. This is also the case for other constructive lattices (k-wheels, k-Möbius ladders) [24,26] obtained by adding diametrical edges to pristine worlds, and for the most economical bipartite graph. Ideal (though virtually unrealizable) constructive graphs do much better: the hypercube is always synchronizable with $f \sim \log_2 n/n$. Similarly, random graphs show

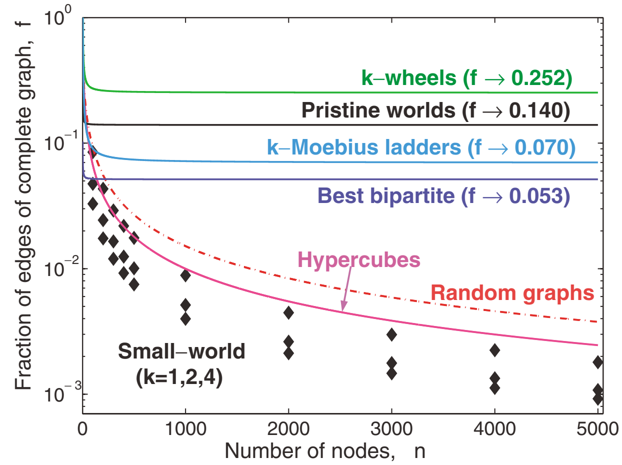

FIG. 3 (color online). Cost (in edges) to synchronize n chaotic x-coupled Rössler systems for different topologies: deterministic graphs (pristine worlds and the related k-wheels and k-Möbius ladders, bipartite graphs, hypercubes), random graphs, and small worlds (◆). Small worlds of low-k scale favorably compared to latticelike structures, to the ideal hypercubes, and to random graphs.

almost sure synchronization when $f \sim \ln n/n$. Remarkably, our numerics in Fig. 3 indicate that the cost of synchronization for SW networks of low k is comparable to or below these ideal examples.

Beyond the potential usefulness of the SW route to improve synchronizability, it is still unclear how this dynamic attribute is related to the small-world definition, which is based on structural properties [1,3]. The SW region is delimited by its onset $s_L \sim 1/n$, given by the decay of the average graph distance [7]; and by its end

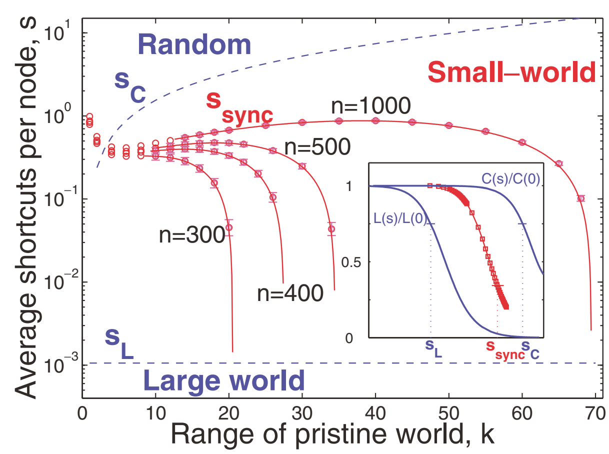

FIG. 4 (color online). Synchronizability thresholds $s_{\mathrm{sync}}(\circ)$ for graphs with n nodes ($n = 300, 400, 500, 1000$) and range $k \in [1, 70]$, averaged over 1000 realizations—solid lines from an analytical perturbation valid in $n^{1/3} < k < k^0_{\mathrm{min}}(n)$. For most parameters, s_{sync} lies within the SW region between the dashed lines (depicted for $n = 1000$), but it is distinct from its onset s_L. Inset: decay of the average distance L, clustering C, and eigenratio (squares) as shortcuts are added to a pristine world of $n = 500$ and $k = 20$. We define s_L and s_C as the points where L and C are 75% of the pristine world value.

$s_C \simeq k(-1 + [(8k-1)/(6k-3)]^{-1/2}) \simeq 0.155k$, marked by the loss of transitivity and clustering that randomizes the graph [27]. A graph is a "small world" when its average distance is small while its clustering is still large. Figure 4 shows that synchronizability is generally achieved within the boundaries of the SW region, albeit with a complicated dependence on the size n and range k of the network. However, the synchronization threshold $s_{\rm sync}$ is distinct, both in value and in scaling, to the onset of SW. Hence, the small-world property does not guarantee synchronizability. Note again the high efficiency of low-k SW networks, which need only $s \sim 1$ shortcuts per node to synchronize [28].

We can gain further insight through an "honest" [29] perturbative analysis of the SW Laplacian $G = G^0 + G^r$, with G^0 the deterministic Laplacian of the pristine world and G^r for the random shortcuts. The stochastic Laplacian matrix G^r (symmetric, null row-sum) is formed from $n(n-2k-1)/2$ independent identically distributed Bernoulli random variables which take the value 1 with probability $q/n \equiv 2s/(n-2k-1)$ (and 0 with probability $1 - q/n$). Skipping the details, we sketch the main results of the stochastic analysis [24]. The expectations of the SW Laplacian eigenvalues are

$$\mathcal{E}\theta_l^{(1)} \simeq q \pm \sqrt{3\pi q/4n}, \quad q \ll n, \quad k \ll n\,, \tag{6}$$

$$\mathcal{E}\theta_1^{(2)} \simeq \frac{-2q}{K^3}\left[\frac{9n}{\pi^2} + K^2 - \left(\frac{7}{5} + \frac{6}{\pi^2}\right)K - \frac{2}{\pi}\right], \tag{7}$$

where $K = 2k+1$, and (7) provides an improved approximation for FNZE. Using (1)–(3), (6), and (7), we obtain $s_{\rm sync}$ from an algebraic equation involving n and k: $\theta_{\max}^0 + \mathcal{E}\theta_{\max}^{(1)} = \beta(\theta_1^0 + \mathcal{E}\theta_1^{(1)} + \mathcal{E}\theta_1^{(2)})$. This approximates well the numerics (Fig. 4) in $n^{1/3} < k \ll n$, the region of validity of the Rayleigh-Schrödinger expansion [30]. Our analysis is consistent with the value $k_{\min}^0$ where the pristine world becomes deterministically synchronizable (i.e., $s_{\rm sync} = 0$). We can also estimate [24] the maximum $s_{\rm sync}^*$ in the region of validity. We find that asymptotically $s_{\rm sync}^* \simeq [2(1 + 2/3\pi)/(2\sqrt{3} - 3)(\beta - 1)]s_C \simeq [5.22/(\beta - 1)]s_C$. The synchronization threshold is linked to the end of the SW region, not to its onset.

These results hint at new connections between graph theory and network dynamics. Remarkably, the eigenratio criterion can be related to other graph-theoretical properties (e.g., connectivity, diameter, and convergence of Markov chains) [22,24,31]. Our work indicates that in aiming at synchronizing systems with a negative region in the master stability function, it is sufficient to look for graphs with eigenratio tending to one. With a view to improved design, additional measures of cost (e.g., robustness under edge deletion or degraded synchronization) should be considered. Other extensions could encompass more general concepts of stability and broader definitions of small worlds [27].

We thank Steve Strogatz for his deep and insightful involvement in this work, and Mark Newman for sharing computer code and unpublished results.

[1] D. J. Watts and S. H. Strogatz, Nature (London) **393**, 440 (1998).
[2] S. H. Strogatz, Nature (London) **410**, 268 (2001).
[3] D. J. Watts, *Small Worlds* (Princeton University Press, Princeton, 1999).
[4] H. Jeong *et al.*, Nature (London) **407**, 651 (2000).
[5] M. Barthelemy and L. Amaral, Phys. Rev. Lett. **82**, 3180 (1999).
[6] A. Barrat and M. Weigt, Eur. Phys. J. B **13**, 547 (2000).
[7] M. E. J. Newman, C. Moore, and D. J. Watts, Phys. Rev. Lett. **84**, 3201 (2000).
[8] M. E. J. Newman and D. J. Watts, Phys. Lett. A **263**, 341 (1999).
[9] C. Moore and M. E. J. Newman, Phys. Rev. E **61**, 5678 (2000).
[10] R. Kulkami, E. Almaas, and D. Stroud, Phys. Rev. E **61**, 4268 (2000).
[11] R. Monasson, Eur. Phys. J. B **12**, 555 (1999).
[12] S. Jespersen, I. Sokolov, and A. Blumen, J. Chem. Phys. **113**, 7652 (2000).
[13] M. Kuperman and G. Abramson, Phys. Rev. Lett. **86**, 2609 (2001).
[14] J. M. Kleinberg, Nature (London) **406**, 845 (2000).
[15] L. F. Lago *et al.*, Phys. Rev. Lett. **84**, 2758 (2000).
[16] X. Wang and G. Chen, Int. J. Bifurcation Chaos Appl. Sci. Eng. **12**, 187 (2002).
[17] P. Gade and C. Hu, Phys. Rev. E **62**, 6409 (2000).
[18] J. F. Heagy, T. L. Carroll, and L. M. Pecora, Phys. Rev. Lett. **74**, 4185 (1995).
[19] L. M. Pecora and T. L. Carroll, Phys. Rev. Lett. **80**, 2109 (1998).
[20] L. M. Pecora, Phys. Rev. E **58**, 247 (1998).
[21] K. Fink *et al.*, Phys. Rev. E **61**, 5080 (2000).
[22] B. Mohar, in *Graph Symmetry: Algebraic Methods and Applications*, NATO ASI, Vol. 497 (Kluwer, Dordrecht, 1997).
[23] The analysis is quite general [21]: it can be extended to eliminate the zero row-sum constraint, and to comprise nonlinear coupling and other synchronization criteria.
[24] M. Barahona and L. M. Pecora (unpublished).
[25] V. Latora and M. Marchiori, Phys. Rev. Lett. **87**, 198701 (2001).
[26] A. Schwenk, *Lecture Notes in Mathematics* (Springer, New York, 1974), Vol. 406, pp. 153–172.
[27] M. E. J. Newman, S. H. Strogatz, and D. J. Watts, Phys. Rev. E **64**, 026118 (2001).
[28] B. Bollobás and F. R. K. Chung, SIAM J. Discrete Math. **1**, 328 (1988).
[29] W. E. Boyce, in *Probabilistic Methods in Applied Mathematics*, edited by A. T. Bharucha-Reid (Academic Press, New York, 1968), pp. 1–73.
[30] The doubly degenerate perturbation is invalid for $k < n^{1/3}$ due to eigenvalue bunching (quasidegeneracy). We are developing another approximation in this limit.
[31] F. R. K. Chung, *Spectral Graph Theory* (AMS, Providence, RI, 1997).